

RESEARCH ARTICLE



Effect of Active Dithiocarbamate Derivatives on Copper Nano Film Deposition

OPEN ACCESS**Received:** 13-01-2023**Accepted:** 10-04-2023**Published:** 28-04-2023

Citation: Balaramesh P, Jayalakshmi S, Anitha V, Fdo A, Venkatesh P (2023) Effect of Active Dithiocarbamate Derivatives on Copper Nano Film Deposition. Indian Journal of Science and Technology 16(17): 1260-1267. <https://doi.org/10.17485/IJST/v16i17.98>

* **Corresponding author.**

pbr.sh@rmkec.ac.in

Funding: None

Competing Interests: None

Copyright: © 2023 Balaramesh et al. This is an open access article distributed under the terms of the [Creative Commons Attribution License](#), which permits unrestricted use, distribution, and reproduction in any medium, provided the original author and source are credited.

Published By Indian Society for Education and Environment ([iSee](#))

ISSN

Print: 0974-6846

Electronic: 0974-5645

P Balaramesh^{1*}, S Jayalakshmi², V Anitha³, Absara Fdo⁴, P Venkatesh⁵

1 Associate Professor, Department of Chemistry, R.M.K. Engineering College, Chennai, 601 206, Tamil Nadu, India

2 Assistant Professor, Department of Chemistry, VISTAS, Chennai, 600 117, Tamil Nadu, India

3 Assistant Professor, Department of Chemistry, Vellammal Engineering College, Chennai, 600 066, Tamil Nadu, India

4 Research Scholar, Department of Chemistry, Pachaiyappa's College, Chennai, 600 030, Tamil Nadu, India

5 Associate Professor, Department of Chemistry, Pachaiyappa's College, Chennai, 600 030, Tamil Nadu, India

Abstract

Objective: The coordination and electrochemistry-related effects and uses of piperidine dithiocarbamate (pipdct) and piperazine dithiocarbamate (pzdct) are the main topics of this article. **Method:** An environment friendly electroless bath was created using a very small amount of biodegradable methanesulphonic bronsted acid, Glyoxylic acid as a reducing agent, Xylitol as a non-toxic natural polyhydroxylic complexing agent and potassium hydroxide as pH modifier. Compact and finer deposits were obtained at pH 13.0 and 45°C with an addition of 1 ppm of pipdct and pzdct in an optimized bath. **Findings:** The inhibiting effect of pipdct and pzdct additives depends on deposit properties, throwing power, thickness uniformity, surface tension and grain structure management. **Novelty:** In this electroless copper plating method, pipdct and pzdct improved the physical properties and produced quality deposits. Gravimetric and weight gain calculations were used to determine the physical parameters. AFM experiments were used to describe the surface morphologies of copper deposits. By using X-ray diffractogram (XRD) analysis, the copper deposits' crystallite sizes were quantified, and cyclic voltammetry analysis was used to assess their quality.

Keywords: Glyoxylic acid; Piperazine dithiocarbamate; Piperidine dithiocarbamate; Surface morphology; Xylitol

1 Introduction

Coordination chemistry is well recognized by the scientific community and has a vast array of uses for coordination molecules⁽¹⁾. The history of organosulfur chemistry began with the invention of dithiocarbamates (DTC). The most researched complexes now are dithiocarbamates and dithiophosphates, due to their biological, agricultural, and industrial fields' reliance on metal chelates and their metal-binding properties⁽²⁾.

Dithiocarbamates are employed for coating along with copper. Since copper dithiocarbamates have been proved to be potential candidates for cancer treatment, PET-imaging and SOD inhibition, the resultant product may be analyzed for possessing biological applications⁽³⁾. In addition, dithiocarbamates also constitute an important class of fungicides, herbicides, and pesticides⁽⁴⁾.

The following are the main benefits of DTCs: (a) metal DTC complexes are more stable than other organic analytical ligands; (b) synthesis requires only one step; (c) preparation in a typical laboratory is convenient; and (d) water solubility is reasonable and can be used to develop solvent miniaturization protocols. The nitrogen atom of the dithiocarbamate complex has a single pair of electrons which plays a larger role in the electron donation process, as the metal oxidation state increases⁽⁵⁾.

Electroless plating is a technique of depositing a noble metal from its salt solution on a catalytically active surface of a less noble metal by employing a suitable reducing agent, without using electrical energy. The reducing agent supplies the electron for the reduction of metallic ion into metal, which is deposited over the substrate surface, with a uniform thin coating⁽⁶⁾. The coating is achieved through metal ion exchange, using chemical reduction in solution and there is no coating build up on corners and projections. These electroless plated coatings can be achieved as nano film coating⁽⁷⁾.

Electroless coating process along with nanochemistry finds more applications in many industrial fields⁽⁸⁾. In other coating processes, the article or samples are produced in micro scale. But electroless coated articles or samples are very smooth, shiny, more compact and can be achieved in nanoscale deposit⁽⁹⁾. Moreover, the physical, electrochemical, and structural properties of the samples can be modified positively⁽¹⁰⁾.

In this current study, xylitol, which is a natural polyhydroxylic compound could provide alternatives to EDTA, that is currently used as complexing agent in electroless baths. They form very stable complexes with copper (II) ions in alkaline solution^(11,12).

The dithiocarbamates have a unique π electron flow from the nitrogen atom to the sulfur atom through a planar delocalized π orbital structure. The metal experiences a substantial donation that causes a high electron density. This unique property of these compounds has been incorporated in this study and hence the use of piperidine dithiocarbamate and piperazine dithiocarbamate as stabilizers makes this study novel, as this has not been used yet by any researchers, in an electroless deposition bath.

Another novelty of work this work has made use of environmentally friendly glyoxylic acid as the reducing agent, replacing conventionally employed, toxic formaldehyde. Glyoxylic acid, on oxidation releases non-toxic carbon dioxide.

Furthermore, xylitol has been employed as complexing agent. The chelating agent xylitol is also having the credit of natural, biodegradable, polyhydroxylic compound that can be visioned as a potential eco-friendly complexing agent.

2 Methodology

2.1 Reagents

The following chemical compounds were obtained from the listed sources and utilised without additional purification. Piperidine (Qualigens), Piperazine (Qualigens), Ammonia solution (Fisher), Carbon- disulphide (S.D. Fine Chem. Ltd), Absolute ethanol (Reid-de-Ham), Dry ether (Qualigens), (Fisher), Xylitol (Qualigens), Copper as methane sulphonate, Glyoxylic acid (Fisher), Potassium hydroxide (Fisher).

Utilizing analytical-grade compounds, eco-friendly electrolytes were prepared. Copper methanesulphonate, xylitol, glyoxylic acid and potassium hydroxide, the pH adjuster (to vary the pH of the bath) were used to carry out the copper electroless deposition. The electroless copper deposition was carried out in a 100 ml beaker and epoxy sheets were used as substrates.

The substrate was polished with fine grit paper, before being washed with double distilled water. A KMnO_4 and H_2SO_4 solution was used to etch the substrate's surface. SnCl_2 solution is used to sensitize the surface and a PdCl_2 solution in HCl is employed to activate it. The experiments were repeated thrice to minimize the errors.

2.2 Calculating the rate of copper deposition using a formula

The following relation was used to determine the rate of deposition (T):

$$\text{Deposition rate } \{\mu\text{m/h}\} T = W \times 10^{-4} / dAt \quad (1)$$

Where W is the mass of the deposit (g), d is the density of the film material (g/cm^3), 'A' is the area of the film coated (cm^2), and 't' is the coating period (h).

The following equation was used to determine the rate of the electroless copper deposit.

$$\text{Rate of deposition } (\mu\text{m/h}) = \text{Thickness} / \text{Deposition time} \quad (2)$$

2.3 Calculating the thickness of copper deposits

$$\text{Thickness } (\mu\text{m}) = W \times 10^{-4} \times 60 / A \times D \quad (3)$$

The difference between the weights before and after plating was used to determine the deposit weight ($w_1 - w_2$).

The thickness was determined using the deposit weight, the overall area of the plating, and the copper density.

$W = (w_1 - w_2) = \text{Weight of deposit (g)}$

$w_1 = \text{Weight after plating (g)}$

$w_2 = \text{Weight before plating (g)}$

A refers to the substrate's overall plated area (cm^2)

D is for density.

Depending upon the nature of the electroless copper bath, the activation energy was calculated by the following equation.

$$E_a = \text{slope} \times 2.303 \times R \quad (4)$$

2.4 Preparation of stock solutions

The necessary amount of metal salt was dissolved in water and sulfuric acid to prepare the 0.1M stock solutions of palladium (II) chloride (25:75). In order to measure the amount of carbon dioxide gas, about 50g of copper carbonate was weighed, transferred into a 500 ml clean beaker, and treated with 60 ml of methanesulphonic acid^(13,14). The solution was diluted using double distilled water and then made up to 250 ml in a standard measuring flask. Filtration was performed to eliminate any oil or suspended contaminants from the solution, before storing in a sanitized container. N/10 of the recommended sodium thio sulphate solution was used to evaluate the copper content present per millilitre of the stock solution.

2.5 Preparation of piperidine dithiocarbamate

The ligand piperidine dithiocarbamate sodium salt (Pipdtc) was synthesized using a reported method with slight modification. In a typical experiment, sodium hydroxide (0.05 mol) was dissolved in 3 mL of water in an ice bath and 30 mL of ethanol was added to it^(15,16). The solution was stirred with the addition of piperidine (0.05 mol) followed by drop-by-drop addition of carbon disulfide (0.05 mol), which yielded the precipitate of the dithiocarbamate sodium salt. The yellow product was collected by filtration, re-dissolved in a minimum amount of methanol and the pure white product was precipitated by adding required volume of diethyl ether^(17,18).

2.6 Preparation of piperazine dithiocarbamate

The ligand piperazine dithiocarbamate was synthesized by addition of 15 mL cold methanolic solution of piperazine, followed by the cold carbon disulfide. After stirring this solution for 4 hrs under ice bath (0-4 °C), the white precipitate obtained was filtered, washed with diethyl ether, and dried in a desiccator over silica gel^(19,20).

2.7 Electrochemical Studies

A common electrochemical analyzer, the CHI-600D Austin USA, was used to obtain cyclic voltammetric curves. Nitrogen gas was used to deaerate the copper methanesulphonate solution⁽²¹⁾. Platinum wire served as the counter electrode, and an Ag/AgCl reference electrode with saturated KCl solution served as the reference electrode. The voltammograms were recorded in the presence of 0.1 M Na_2SO_4 as the supporting electrolyte at room temperature. Standard glassy carbon electrode was employed as the working electrode, and voltammograms were obtained in the range of -1.2 to +0.5 V at a potential scanning rate of 50 mVs^{-1} . The system can be matched with the electrical equivalent circuit shown below⁽²²⁾.

2.8 Characterization of coating surface

To examine the surface roughness of the Cu deposits, an atomic force microscope (AFM) (NanoSurf Easy Scan2, Switzerland) was employed. To determine the structural characteristics of the copper deposits, X-ray diffraction technique (X'Pert-Pro, P-analytical) was employed. The Debye-Scherrer equation for calculating the particle size is given by,

$$D = K \lambda / \beta \cos \theta \quad (5)$$

2.9 DC Tafel polarization as an electrochemical monitoring method (TP)

Tafel curves are obtained by graphing the current logarithm ($\log I$) against potential and extrapolating the currents in the two Tafel areas. The Tafel plots provide a measurement of the copper salt reduction current, which is equivalent to glyoxylic acid oxidation current. With the knowledge of I_{corr} , Faraday's law may be used to determine the rate of corrosion in the desired units. The classical work of Stern and Geary serves as the foundation for the contemporary methodologies for measuring corrosion rates⁽²³⁾.

$$R_p = \beta_a \times \beta_c / 2.303 (\beta_a + \beta_c) I_{corr} \quad (6)$$

2.10 Electrochemical impedance spectroscopy as a monitoring tool (EIS)

In-depth research on the corrosion phenomena has been performed using the AC impedance method. The perturbation of the working electrode is reduced by providing a low amplitude oscillating potential, and helpful details on the electrochemical properties of the corrosion process on the surface are discovered. For characterizing coated metal surfaces, this approach is a potential tool. In order to study the interfacial charge transfer between an electrolyte and a solid conductor (the working electrode, WE), impedance spectroscopy (EIS), a conventional approach, is very much essential in the field of electrochemical research and electrochemistry⁽²⁴⁾.

C_1 & C_2 – Double layer capacitances,

R_1 & R_2 – Charge transfer resistances

$$C_1 / R_1 + C_2 / R_2 \quad (7)$$

Nyquist diagram {Im (Z) Vs Re (Z')}

$$f_{c1} = 1 / 2\pi R_1 C_1 \text{ and } f_{c2} = 1 / 2\pi R_2 C_2 \quad (8)$$

The sample is exposed to a small-amplitude signal (between 5 and 50 mV), over a range of frequencies from 10 MHz to 10 kHz, in order to perform an EIS test. The EIS instrument records the actual (resistance) and fictitious (capacitance) components of the system's impedance response⁽²⁵⁾.

3 Results and discussion

All stabilizers form stable complexes with copper methanesulphonate above pH 12.0. For the xylitol based plain bath, the rate of copper deposition starts at pH 12.5, reaches a maximum at 13.25, and is stable up to pH 13.0 and the baths show optimum deposition at different pH values. In addition to this, the stability of the bath was also determined at various temperatures. The deposition rate is observed to increase with increase in temperature of the bath until 60°C and produces thin crystalline film of Cu.

Although the deposition rate is high at above 60 °C, the deposits are unstable and are not crystalline. The whole bath reaction is accelerated to an extent, that the deposition reaction comes to a completion within a few hours viz., 3–5 h. So, the optimum temperature for xylitol PB with pipdte and pzdte stabilizers is fixed at 45°C. The activation energy is another marker to understand the nature of the bath. The activation energy was calculated from the slope of the plot of $\log r$ vs. $1/T$. In general, the activation energy is inversely proportional to the deposition rate. Based on this condition, activation energy decreases from xylitol PB to pzdte. Table 1 shows that the thickness of the deposits increases on increasing the plating time. The thickness value is found to gradually increase from xylitol PB to pzdte. This trend is analogous to the deposition rate. After several experiments to decide the stability conditions, the bath was optimized at 3 g/L of copper methanesulphonate, 10 g/L of glyoxylic acid, and pH 13.00 at 45 °C.

Table 1. Influence of various physical properties of xylitol PB with pipdte and pzdte stabilizers

Xylitol PB with Dithiocarbamate Stabilizer	Physical properties		
	Deposition rate	Thickness	Activation energy
Xylitol PB	3.02	181.2	70.2
pipdte (1ppm)	2.78	166.8	72.6
pzdte (1ppm)	2.62	157.2	73.8

By using cyclic voltammetry, electrochemical properties were investigated, in order to comprehend the impact of the

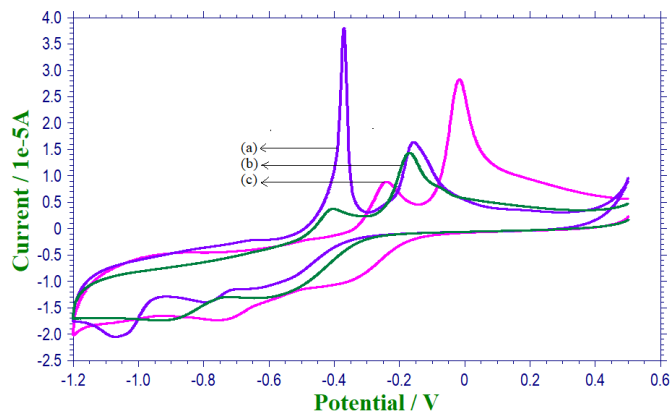


Fig 1. Cyclic voltammogram for electroless Cumethanesulfonate for (a) Xylitol PB, (b) pipdte (1ppm), and (c) pzdte (1ppm)

Table 2. Values of copper deposits in cyclic voltammetry and Tafel studies of xylitol PB with pipdte and pzdte stabilizers

Xylitol PB with Dithiocarbamate Stabilizer	Electrochemical properties			
	CV			Tafel
	E _{pa-1}	I _{pa-1} x10-6	I _{corr}	Deposition Rate
Xylitol PB	-0.2210	3.054	50.64	0.670
pipdte (1ppm)	-0.2468	3.468	44.26	0.472
pzdte (1ppm)	-0.2628	3.522	42.18	0.428

complexing agents on the number and quality of copper deposits in the copper methanesulphonate bath. The values of the anodic peak potential and anodic peak current were being affected by charge density, steric variables, etc. Figures 1 and 2 and Table 3 show that the E_{pa-1} values drop as we go from xylitol PB to pzdte, which reflects the quality of the copper deposits, according to the cyclic voltammogram for electroless Cu methanesulphonate systems, i.e., (a) xylitol PB (b) pipdte, and (c) pzdte -containing electroless coating. The lowest E_{pa-1} value (V) is shown by pzdte, while Xylitol plain bath exhibits a greater E_{pa-1} value (-0.2210 V) than pipdte.

Table 3. Values of copper deposits in impedance studies of xylitol PB with pipdte and pzdte stabilizers

Xylitol PB with Dithiocarbamate Stabilizer	Electrochemical properties (Impedance)			
	Double layer Capacitance (Cdl)(μF/cm ²)		Charge transfer Resistance (Rt)(mΩ/cm ²)	
	C1x10-6	C2x10-3	R1	R2
Xylitol PB	3.274	0.1521	265	32.23
pipdte (1ppm)	4.628	2.216	462	52.42
pzdte (1ppm)	6.126	3.209	558	69.12

The atomic force microscope was used to determine the roughness value and shape of the deposits and X-ray diffraction (XRD) examinations were used to measure the crystallite size and specific surface area.

For all the three baths, an AFM image of a Cu thin film, a 3D image and the surface topography were recorded.

Table 4. Influence of surface morphologies on Xylitol PB, pipdte and pzdte

Xylitol PB with Dithiocarbamate Stabilizer	Surface morphologies		
	AFM	XRD	
	Roughness value (nm)	Crystallite size (nm)	Specific surface area (m ² / g)
Xylitol PB	216	121	5.534
pipdte (1ppm)	108	92	7.279
pzdte (1ppm)	96	78	8.585

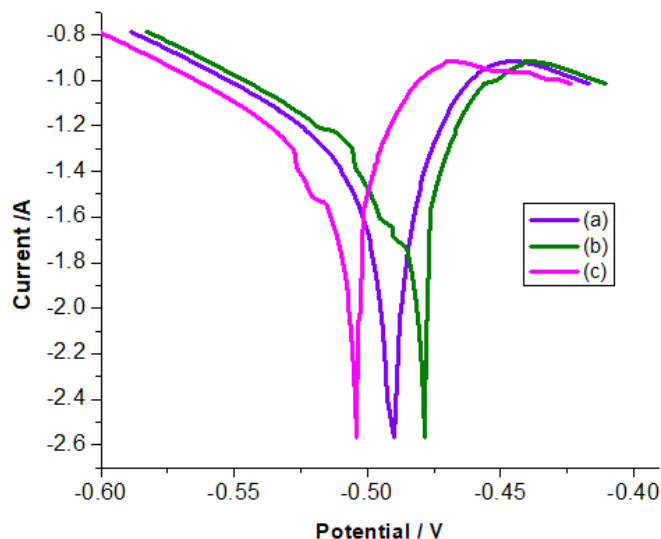


Fig 2. Tafel polarization curve for electroless copper (a) Xylitol PB, (b) pipdte (1ppm), and (c) pzdtc (1ppm)

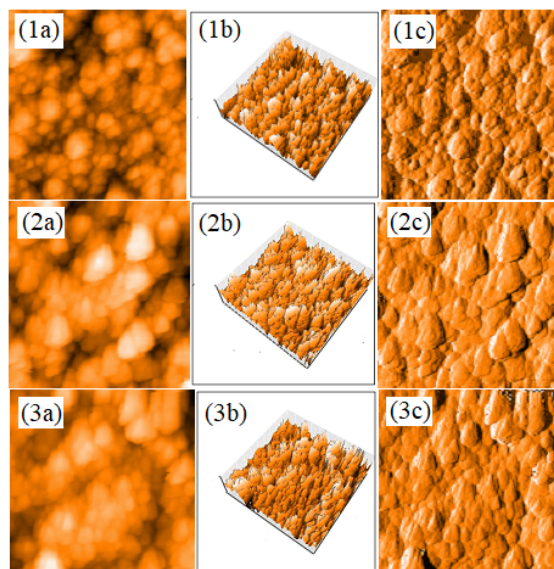


Fig 3. AFM images of (a) Xylitol PB, (b) pipdte (1ppm), and (c) pzdtc (1ppm) (a) electroless coating topography of copper deposits, (b) 3D image, (c) surface area

The surface appearances of the deposits are influenced by the additives. Soft sulphur donor atoms in pipdte and pzdtc effectively form a four-member ring during chelation by easily complexing with the soft copper ion. These compounds also react with metal ions of the bi-, tri- and tetravalent types to create chelates known as "bis," "tris," and "tetrakis," respectively.

Due to the electrical resonance in the $-NCS_2$ moiety of the ligand, the chelate ring complexes are stable. The stability of the ring is also improved by the back donation of electrons from the metal to the complexing agent and the colour of the complexes is due to the transition of the S-C-N and S-C-S chromophores.

Due to the movement of electrons from alkyl group to nitrogen and subsequently to donor center via carbon by inductive (+I effect) and conjugation processes, a partial double bond character is also anticipated to form between carbon and nitrogen. Because of its high conductivity and solubility, which leads to the (200) plane, copper methanesulphonate produces more copper ions than other baths.

As a result, all the electroless baths exhibit the (200) planes favoured orientation. Specific surface area values are inversely related to crystallite size and proportionate to line width (FWHM) values. The structural characteristics of deposits obtained from baths containing complexing agent and additives are studied in this investigation.

4 Conclusion

- In a copper methanesulphonate bath used for electroless copper deposition, piperidine dithiocarbamate (pipdctc) and piperazine dithiocarbamate (pzdctc) were utilised and the effects of the novel additives on the nature and rate of deposition were investigated.
- KOH was used as the pH adjuster and to increase the solubility of the by-products during electroless copper deposition. The additives pipdctc and pzdctc acted as stabilizers and effective corrosion inhibitors in the alkaline medium.
- All the autocatalytic baths were found to exhibit optimum deposition at a pH of 13.00 ± 0.25 . Optimum Cu deposition was seen at a temperature of 45°C .
- The activation energy, crystallite size and roughness values decreased from xylitol PB to pzdctc. However, the deposition rate, thickness, specific surface area and anode peak potential value increased from xylitol PB to pzdctc.
- Charge density, steric factor, delocalized π electron, inductive effect, conjugation effect, and presence of hetero atoms (sulfur and nitrogen) in the complexing agents were found to significantly influence the surface morphologies of the copper deposits.
- This research work has made use of biologically potent dithiocarbamates that are generally used for cancer treatment, PET-imaging, and SOD inhibition. Therefore, the resultant copper dithiocarbamate coated epoxy surface may also be employed in instruments or techniques that involve cancer treatment and PET-imaging.
- The utilization of dithiocarbamates in electroless deposition bath is a new attempt which has not been tried by any research experts in their deposition process and hence it finds novelty in this current study.

References

- 1) Ajiboye TO, Ajiboye TT, Marzouki R, Onwudiwe DC. The Versatility in the Applications of Dithiocarbamates. *International Journal of Molecular Sciences*. 2022;23(3):1317–1317. Available from: <https://doi.org/10.3390/ijms23031317>.
- 2) Tan YS, Yeo CI, Tiekink ERT, Heard PJ. Dithiocarbamate Complexes of Platinum Group Metals: Structural Aspects and Applications. *Inorganics*. 2021;9(8):60–60. Available from: <https://doi.org/10.3390/inorganics9080060>.
- 3) Ayalew ZM, Zhang X, Guo X, Ullah S, Leng S, Luo X, et al. Removal of Cu, Ni and Zn directly from acidic electroplating wastewater by Oligo-Ethyleneamine dithiocarbamate (OEDTC). *Separation and Purification Technology*. 2020;248:117114–117114. Available from: <https://doi.org/10.1016/j.seppur.2020.117114>.
- 4) Zeng Q, Hu S, Zheng W, He Z, Zhou L, Huang Y. Spongy Crosslinked Branched Polyethylenimine-Grafted Dithiocarbamate: Highly Efficient Heavy Metal Ion-Adsorbing Material. *Journal of Environmental Engineering*. 2020;146(2). Available from: [https://doi.org/10.1061/\(ASCE\)EE.1943-7870.0001638](https://doi.org/10.1061/(ASCE)EE.1943-7870.0001638).
- 5) de la Calle I, Ruibal T, Lavilla I, Bendicho C. Direct immersion thin-film microextraction method based on the sorption of pyrrolidine dithiocarbamate metal chelates onto graphene membranes followed by total reflection X-ray fluorescence analysis. *Spectrochimica Acta Part B: Atomic Spectroscopy*. 2019;152:14–24. Available from: <https://doi.org/10.1016/j.sab.2018.12.005>.
- 6) Duran-García EI, Martínez-Santana J, Torres-Gómez N, Vilchis-Nestor AR, García-Orozco I. Copper sulfide nanoparticles produced by the reaction of N-alkyldithiocarbamatecopper(II) complexes with sodium borohydride. *Materials Chemistry and Physics*. 2021;269:124743–124743. Available from: <https://doi.org/10.1016/j.matchemphys.2021.124743>.
- 7) de Freitas Oliveira JW, Rocha HAO, de Medeiros WMTQ, Silva MS. Application of Dithiocarbamates as Potential New Antitrypanosomatids-Drugs: Approach Chemistry, Functional and Biological. *Molecules*. 2019;24(15):2806–2806. Available from: <https://doi.org/10.3390/molecules24152806>.
- 8) Wang H, Wei J, Jiang H, Zhang Y, Jiang C, Ma X. Design, Synthesis and Pharmacological Evaluation of Three Novel Dehydroabietyl Piperazine Dithiocarbamate Ruthenium (II) Polypyridyl Complexes as Potential Antitumor Agents: DNA Damage, Cell Cycle Arrest and Apoptosis Induction. *Molecules*. 2021;26(5):1453–1453. Available from: <https://doi.org/10.3390/molecules26051453>.
- 9) Adeyemi JO, Onwudiwe DC. The mechanisms of action involving dithiocarbamate complexes in biological systems. *Inorganica Chimica Acta*. 2020;511:119809–119809. Available from: <https://doi.org/10.1016/j.ica.2020.119809>.
- 10) Mansouri G, Ghobadi M, Notash B. Synthesis, spectroscopic, structural, DFT and antibacterial studies of cyclometalated rhodium(III) complex based on morpholinedithiocarbamate ligand. *Inorganic Chemistry Communications*. 2021;130:108707–108707. Available from: <https://doi.org/10.1016/j.inoche.2021.108707>.
- 11) Balaramesh P, Jayalakshmi S, Fdo SA, Anitha V, Venkatesh P. Thin film to nano copper deposition by special additives on an ecofriendly electroless bath. *Materials Today: Proceedings*. 2021;47(9):1862–1867. Available from: <https://doi.org/10.1016/j.matpr.2021.03.513>.
- 12) Dev A, Tandon S, Jha P, Singh P, Dutt A. Investigation of process parameters in electroless copper plating on polystyrene. *Sādhanā*. 2020;45(156). Available from: <https://doi.org/10.1007/s12046-020-01377-3>.
- 13) Ajiboye TO, Oluwarinde BO, Montso PK, Ateba CN, Onwudiwe DC. Antimicrobial activities of Cu(II), In(III), and Sb(III) complexes of N-methyl-N-phenyl dithiocarbamate complexes. *Results in Chemistry*. 2021;3:100241–100241. Available from: <https://doi.org/10.1016/j.rechem.2021.100241>.
- 14) Odularu AT, Ajibade PA. Dithiocarbamates: Challenges, Control, and Approaches to Excellent Yield, Characterization, and Their Biological Applications. *Bioinorganic Chemistry and Applications*. 2019;2019:1–15. Available from: <https://doi.org/10.1155/2019/8260496>.

- 15) Al-Janabi ASM, Kadhim MM, Al-nassiry AIA, Yousef TA. Antimicrobial, computational, and molecular docking studies of Zn (II) and Pd (II) complexes derived from piperidine dithiocarbamate. *Applied Organometallic Chemistry*. 2021;35(2):e6108–e6108. Available from: <https://doi.org/10.1002/aoc.6108>.
- 16) Salman MM, Al-Dulaimi AA, Al-Janabi ASM, Alheety MA. Novel dithiocarbamate nano Zn(II), Cd(II) and Hg(II) complexes with pyrrolidinedithiocarbamate and N,N-diethyldithiocarbamate. *Materials Today: Proceedings*. 2021;43(2):863–868. Available from: <https://doi.org/10.1016/j.matpr.2020.07.082>.
- 17) Mohammadi I, Shahrabi T, Mahdavian M, Izadi M. Cerium/diethyldithiocarbamate complex as a novel corrosion inhibitive pigment for AA2024-T. *Scientific Reports*. 2020;10(5043):1–15. Available from: <https://doi.org/10.1038/s41598-020-61946-8>.
- 18) Wang H, Wei J, Jiang H, Zhang Y, Jiang C, Ma X. Design, Synthesis and Pharmacological Evaluation of Three Novel Dehydroabietyl Piperazine Dithiocarbamate Ruthenium (II) Polypyridyl Complexes as Potential Antitumor Agents: DNA Damage, Cell Cycle Arrest and Apoptosis Induction. *Molecules*. 2021;26(5):1453–1453. Available from: <https://doi.org/10.3390/molecules26051453>.
- 19) Shin A, Kim BK, Kim M, Jeong M, Lee D, Ha H, et al. Microstructural and physicochemical origins of electroless copper deposition on graphite enhanced by acid pretreatment. *Materials Chemistry and Physics*. 2023;295:127118–127118. Available from: <https://doi.org/10.1016/j.matchemphys.2022.127118>.
- 20) Pastrana-Dávila A, Amaya-Flórez A, Aranaga C, Ellena J, Macías M, Flórez-López E, et al. Synthesis, characterization, and antibacterial activity of dibenzildithiocarbamate derivatives and Ni(II)–Cu(II) coordination compounds. *Journal of Molecular Structure*. 2021;1245:131109–131109. Available from: <https://doi.org/10.1016/j.molstruc.2021.131109>.
- 21) Adeyemi JO, Onwudiwe DC. The mechanisms of action involving dithiocarbamate complexes in biological systems. *Inorganica Chimica Acta*. 2020;511:119809–119809. Available from: <https://doi.org/10.1016/j.ica.2020.119809>.
- 22) Kadhim MM, Juber LAA, Al-Janabi ASM. Estimation of the Efficiency of Corrosion Inhibition by Zn-Dithiocarbamate Complexes: a Theoretical Study. *Iraqi Journal of Science*. 2021;62(9):3323–3335. Available from: [https://doi.org/10.24996/ijs.2021.62.9\(SI\).3](https://doi.org/10.24996/ijs.2021.62.9(SI).3).
- 23) Huang JH, Shih PS, Renganathan V, Gräfner SJ, Chen YA, Huang CH, et al. Development of high copper concentration, low operating temperature, and environmentally friendly electroless copper plating using a copper - glycerin complex solution. *Electrochimica Acta*. 2022;425:140710–140710. Available from: <https://doi.org/10.1016/j.electacta.2022.140710>.
- 24) Mohammadi I, Shahrabi T, Mahdavian M, Izadi M. Cerium/diethyldithiocarbamate complex as a novel corrosion inhibitive pigment for AA2024-T3. *Scientific Reports*. 2020;10(5043):1–15. Available from: <https://doi.org/10.1038/s41598-020-61946-8>.
- 25) Hui WQ, Song LX. Study on new process of electroless copper plating pretreatment on carbon fiber surface. *Materials Research Express*. 2023;10(2):1–8. Available from: <https://doi.org/10.1088/2053-1591/acac02>.